



Article

Concurrent Climate Extremes and Impacts on Ecosystems in Southwest China

Lulu Liu ¹, Yuan Jiang ^{1,2}, Jiangbo Gao ^{1,*}, Aiqing Feng ³, Kewei Jiao ⁴, Shaohong Wu ^{1,2}, Liyuan Zuo ^{1,2}, Yuqing Li ^{1,2} and Rui Yan ^{1,2}

¹ Key Laboratory of Land Surface Pattern and Simulation, Institute of Geographic Sciences and Natural Resources Research, Chinese Academy of Sciences, Beijing 100101, China; liull.16b@igsnr.ac.cn (L.L.); jiangy.18s@igsnr.ac.cn (Y.J.); wush@igsnr.ac.cn (S.W.); zuoly.17s@igsnr.ac.cn (L.Z.); liyq.19b@igsnr.ac.cn (Y.L.); yanr.20b@igsnr.ac.cn (R.Y.)

² College of Resources and Environment, University of Chinese Academy of Sciences, Beijing 100049, China

³ National Climate Center, China Meteorological Administration, Beijing 100081, China; fengaq@cma.gov.cn

⁴ Key Laboratory of Forest Ecology and Management, Institute of Applied Ecology, Chinese Academy of Sciences, Shenyang 110016, China; jiaokewei@iae.ac.cn

* Correspondence: gaojiangbo@igsnr.ac.cn

Abstract: Global warming and its associated changes in temperature and precipitation have significantly affected the ecosystem in Southwest China, yet studies that integrate temperature and precipitation changes are inadequate for quantitatively assessing the impacts of extreme events on ecosystems. In this study, the return period of concurrent climate extremes characterized by precipitation deficit and extreme temperature and the spatial and temporal dynamic patterns of their impacts on ecosystems were assessed by using high-precision temperature and precipitation data, as well as NDVI and NPP data collected for the 1985–2015 period. The results show that the 2009 concurrent event had a return period of about 200 years. The return periods of individual climate factors are significantly overestimated or underestimated. Concurrent events significantly reduced the spring and annual Normalized Difference Vegetation Index (NDVI) and net primary productivity (NPP) in Southwest China. The magnitude of the reduction in vegetation greenness and productivity increased with the intensity of concurrent events. Concurrent events beginning in autumn 2009 reduced spring NDVI and NPP by 8.8% and 23%, and annual NDVI and NPP by 2.23% and 7.22%, respectively. Under future climate scenarios, the return period of concurrent events could be significantly shortened, which would have a more severe impact on regional ecosystems.

Keywords: concurrent events; return period; precipitation deficit; NDVI; NPP; Southwest China



Citation: Liu, L.; Jiang, Y.; Gao, J.; Feng, A.; Jiao, K.; Wu, S.; Zuo, L.; Li, Y.; Yan, R. Concurrent Climate Extremes and Impacts on Ecosystems in Southwest China. *Remote Sens.* **2022**, *14*, 1678. <https://doi.org/10.3390/rs14071678>

Academic Editors: Tsegaye Tadesse, John J. Qu, Manuela Balzarolo and Frank Veroustraete

Received: 25 December 2021

Accepted: 29 March 2022

Published: 31 March 2022

Publisher's Note: MDPI stays neutral with regard to jurisdictional claims in published maps and institutional affiliations.



Copyright: © 2022 by the authors. Licensee MDPI, Basel, Switzerland. This article is an open access article distributed under the terms and conditions of the Creative Commons Attribution (CC BY) license (<https://creativecommons.org/licenses/by/4.0/>).

1. Introduction

Climate change and extreme weather and climate events are among the most serious natural disasters affecting the social economy, agriculture, and ecosystems [1]. In the context of climate change and socio-economic development, the frequency and intensity of extreme weather and climate events will increase in the future. Climate change will directly increase the probability of extreme warming events, and is also expected to increase the probability of drought events [2]. At the same time, climate change has greatly increased the probability of the simultaneous occurrence of heatwaves and droughts [3], such as Cohen et al. [4] found that extreme weather, including heatwaves, droughts, and high rainfall, is becoming more common and affecting a diversity of species and taxa. Weilhammer et al. [5] pointed out that due to climate change, the frequency, intensity and severity of extreme weather events, such as heat waves, cold waves, and droughts, are increasing, which could adversely affect human health. There have been many separate studies on drought and heatwaves in the context of climate change, but studies focusing on the hazards and impacts of droughts and heatwaves are still scarce.

Some studies have qualitatively and quantitatively calculated the impact of drought events on ecosystems; for example, Nanzad et al. [6] quantitatively analyzed the impacts of drought on the NPP of Mongolian terrestrial ecosystems. Li et al. [7] identified the spatial relationship between droughts and the terrestrial ecosystem productivity as being crucial for enhancing ecosystem services in China. These studies explored the trend of NPP changes under the influence of drought, and clarified the fact that ecosystems are often affected by drought events. Heatwaves also have a greater impact on ecosystem changes [8]. For example, Ainsworth et al. [9] assessed the merits of proposed ecological interventions due to heatwaves. With the application of long-term meteorological observation, scenario simulation, and remote sensing data, global and regional studies have shown that ecosystems are affected by extreme events such as droughts and heatwaves [10]. However, quantitative analysis of ecosystem changes caused by extreme events is still insufficient, and the effects of concurrent events of droughts and heatwaves on ecosystems are less well studied.

A terrestrial ecosystem is a land-based community of organisms and the interactions of biotic and abiotic components in a given area. Climate change has had and will continue to have profound impacts on the structure and function of terrestrial ecosystems, particularly in ecologically vulnerable regions [11,12]. Southwest China is the largest continuous area and the most ecologically vulnerable region in China due to the wide distribution of karst [13]. Southwest China mostly comprises rocky desertification areas, soil erosion areas, and poverty-stricken population areas [14]. In Southwest China, karst areas are widespread, with shallow soils, poor continuity, and low land productivity [15]. Studies have shown that Southwest China is very sensitive to climate change, with frequent occurrences of droughts and heatwaves, and the increasing demand for water resources for regional development has exacerbated the impact of extreme events [16]. The Enhanced Vegetation Index (EVI) for vegetation in Southwest China shows a fluctuating trend of increase and correlates well with temperature and precipitation over the same period, both of which are mainly positive [17]. The frequency of extreme events in Southwest China has increased significantly over the past few decades [18]. In 2009, Southwest China suffered from extremely severe consecutive droughts in autumn, winter and spring. The reason for this drought was low precipitation and high temperature, both of which worked together and had a greater impact on the local ecosystem [19,20].

The return period is an important means for measuring the risk level of extreme events [21]. The commonly used extreme value distribution models mainly assess the hazard level of individual indicator variables but struggle to accurately measure the hazard and the consequent risk of concurrent events [22,23]. As the field develops, multivariate coordination methods are increasingly being used in climate change research to study the return period of concurrent events [24]. On this basis, research on the impact of concurrent events on natural and social economic systems can be carried out. To the best of our knowledge, few studies have attempted to conduct research on the impact of concurrent droughts and heatwaves on the ecosystem in Southwest China, and even less work has been conducted to reflect the full chain of climate change-concurrent events–ecological risk quantitative assessment. Therefore, starting with the extreme events in Southwest China in 2009, we studied the risk assessment of concurrent events of precipitation deficit and extreme temperature, and used NDVI and NPP as indicators to quantitatively evaluate the impact of concurrent events on the ecosystem. This is of great significance for understanding and identifying the comprehensive effects of concurrent events on natural and social economic systems and quantitatively assessing ecosystem risks.

2. Materials and Methods

2.1. Study Region

In recent decades, with climate warming, drought disasters have occurred frequently in Southwest China. The areas with the most severe drought intensity and losses are mainly distributed in southern Sichuan Province, Yunnan Province, and western Guizhou

Province [25,26], and this pattern will continue in the future [27]. In order to objectively select the scope of the study region, this paper conducts a spatial analysis on the anomaly percentage of the most typical concurrent event in 2009. From the autumn of 2009 to the spring of 2010, a severe drought that lasted for more than half a year occurred in Southwest China. According to official statistics, the drought affected more than 64.2 million people, with more than 1.1 million hectares of crop failure and direct economic losses of more than CNY 24.6 billion. Among them, the Yunnan, Guizhou, and Guangxi provinces (autonomous regions) had the most serious drought conditions. In this study, the area with the most severe precipitation deficit conditions (precipitation anomaly percentage $< -50\%$) during this event was selected as the study region (Figure 1), and the study period was selected from October to March of the event development stage [28]. This area is generally consistent with the spatial distribution of major past and future extreme drought events in Southwest China, and is spatially representative and typical of extreme climate events in Southwest China [29,30]. The study region covers an area of approximately 450,000 km², with vegetation dominated by woodland, grassland, and cropland, with average temperatures of 9–12 °C and precipitation of 200–300 mm in winter and spring. This study region was selected with the consideration of highlighting the typicality of the occurrence and ecological impacts of concurrent events, and the time period was selected with the main consideration of promoting awareness of the importance of disasters and their consequences in the winter and spring seasons in Southwest China.

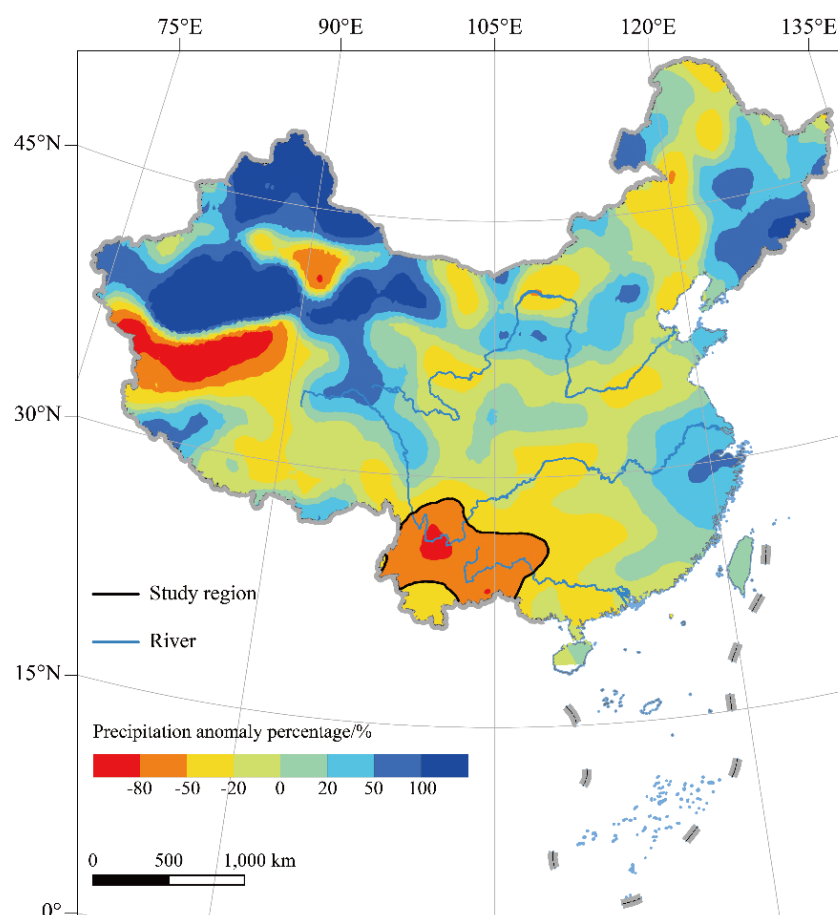


Figure 1. Location of the study region and precipitation anomaly percentage from October 2009 to March 2010 relative to the 1971–2000 period based on CRU data.

2.2. Data

Monthly variables of temperature and precipitation were used in this study to assess the return period of concurrent events of precipitation deficit and extreme temperature.

The observed temperature and precipitation variables were obtained from the China Meteorological Data Service Centre's Dataset of gridded monthly temperature/precipitation in China (Version 2.0) (1961–2018). This is a $0.5^\circ \times 0.5^\circ$ grid dataset established by The National Meteorological Information Center, based on the basic meteorological data of more than 2400 national ground stations, using thin-plate splines and introducing digital elevation data to eliminate the influence of elevation on spatial interpolation accuracy under the unique terrain conditions of the region as much as possible. In view of the insufficient length of the observed data time series, this study also introduced the high-resolution gridded datasets (CRU TS Version 4.03) from The Climatic Research Unit (CRU) at the University of East Anglia (UEA) as a data supplement [31]. CRU TS provides monthly data on a $0.5^\circ \times 0.5^\circ$ grid covering land surfaces (except Antarctica) from 1901 to 2018, and the variables used in this study are temperature and precipitation. The climate scenario data were derived from a daily dataset at a spatial resolution of $0.5^\circ \times 0.5^\circ$ from down-scaled simulations of global climate models (GCMs, i.e., GFDL-ESM2M, HadGEM2-ES, IPSL-CM5A-LR and NorESM1-M) in the framework of the Inter-Sectoral Impact Model Inter-comparison Project (ISI-MIP) for the period from 1950 to 2099 [32]. RCP4.5 and RCP8.5 scenarios were selected to characterize moderate development pathways and high emission pathways, and then monthly temperature and precipitation variables were calculated to match the temporal resolution of the observed data for subsequent analyses and calculations. Observational data and CRU data were also used and analyzed for comparison to ensure accuracy, consistency, and reliability. Together with climate scenario data, this ensured that the data is complete and up to date.

The net primary productivity (NPP) and Normalized Difference Vegetation Index (NDVI) datasets were used to assess the impact of concurrent events on ecosystem productivity in Southwest China. NPP data were derived from the monthly net primary productivity 1 km raster dataset of terrestrial ecosystems in China (1985–2015) provided by Chen et al. [33]. This dataset used the Carnegie-Ames-Stanford Approach (CASA) model with input data including soil data, meteorological data (monthly radiation, precipitation, and temperature values), land cover data, and vegetation index data. In addition, since the distributions of the vegetation types are mainly influenced by the weather, soil, and topographical conditions, the aspect data were also collected, as well as soil and meteorological data. Overall, the NPP data has a high accuracy for regional-scale ecosystem assessment [34]. The NDVI data were obtained from monthly values processed by Jiao et al. [35] using the maximum value composite (MVC) method with a spatial resolution of 8 km. The raw data were obtained from the Global Inventory Monitoring and Modeling Studies (GIMMS) for the period from 1982 to 2015. The simultaneous use of NDVI and NPP data also ensures the reliability and consistency of the ecosystem impact assessment.

2.3. Methods

This study focused on Southwest China, where drought disasters are becoming more serious under the conditions of global warming (Section 2.1), and used datasets including climatic variables, NDVI, and NPP variables (Section 2.2). This study used return period analysis to determine the severity of concurrent events (Section 2.3.2) on the basis of determining the availability of data (Section 2.3.1). The impact of concurrent events on the ecosystem was quantitatively assessed by comparing the change in NDVI and NPP across return periods (Section 2.3.3). The method in Section 2.3.2 was also used to study the possible trends of concurrent events under RCP4.5 and RCP8.5 scenarios, and to infer the possible evolution of the ecosystem in Southwest China in the future.

2.3.1. Accuracy Measurement Indicator and Method

Given the short duration of the time series of observed climate variables, CRU TS datasets were introduced in this study to more accurately describe the severity of concurrent events. It was first necessary to verify the accuracy of CRU data for the study region and to understand the long-term variability characteristics of regional-scale temperature

and precipitation, which was essential for the subsequent regional-scale assessment of concurrent events and their consequences.

First, considering the time series of climate observations and scenario data, the average of 1971–2000 was chosen as the climate mean state in this study.

Subsequently, anomalies in temperature and precipitation for October–March of each year from observational data and CRU data were calculated relative to the mean values for the period.

Finally, to test the accuracy of CRU data, with reference to Zhao et al. [36], the mean absolute error (MAE), mean absolute percentage error (MAPE), root mean square error (RMSE), and correlation coefficient (Pearson's R) between CRU data and observed data were selected as indicators to assess the precision in this study. These assessment metrics have different classifications and can be corresponded to hydrological model accuracy assessment metrics such as Percent bias (PBIAS), Nash-Sutcliffe efficiency (NSE) and Kling-Gupta efficiency (KGE), respectively [37,38].

$$\text{MAE} = \frac{1}{N} \sum_{i=1}^N |C_i - O_i| \quad (1)$$

$$\text{MAPE} = \frac{100\%}{N} \sum_{i=1}^N \left| \frac{C_i - O_i}{O_i} \right| \quad (2)$$

$$\text{RMSE} = \sqrt{\frac{1}{N} \sum_{i=1}^N \left(\frac{C_i - O_i}{O_i} \right)^2} \quad (3)$$

$$R = \frac{\sum_{i=1}^N (C_i O_i) - \frac{1}{N} \sum_{i=1}^N C_i \sum_{i=1}^N O_i}{\sqrt{\left(\frac{1}{N} \sum_{i=1}^N C_i^2 - \frac{(\sum_{i=1}^N C_i)^2}{N} \right) \left(\frac{1}{N} \sum_{i=1}^N O_i^2 - \frac{(\sum_{i=1}^N O_i)^2}{N} \right)}} \quad (4)$$

In Equations (1)–(3), C_i is the CRU value in year i , O_i is the observed value in year i , and N is the total number of years.

2.3.2. Return Period Analysis of Concurrent Climate Extremes

A copula function is a multivariate function obeying uniform distribution over $[0, 1]$, which can be applied to multidimensional joint distribution construction. The advantage of this function is that it is not necessary to assume the same edge function, and it is possible to derive the joint distribution function for various edge distributions, which has a wide range of applications. Common univariate risk estimation methods significantly underestimate or overestimate the return period, which also demonstrates the importance of concurrent climate extremes [39].

Based on Sklar's theorem [40], let F be a two-dimensional distribution function, with univariate margins F_1 and F_2 for random variables X (precipitation) and Y (temperature), and then the copula function (C) is cloud formulated as:

$$F(X, Y) = C(F_1(X), F_2(Y)) \quad X, Y \in R \quad (5)$$

where $F(x)$ is a univariate marginal distribution function.

Based on the marginal distributions $F_1(X)$ and $F_2(Y)$ of the variables X and Y , respectively, the joint distribution of the copula functions of the two variables can be expressed as:

$$F(x, y) = P(X \leq x, Y \leq y) \quad (6)$$

The univariate recurrence period is:

$$T(x) = \frac{1}{1 - F_1(X)} \quad T(y) = \frac{1}{1 - F_2(Y)} \quad (7)$$

For this study, we were interested in the joint return period of the two variables in the concurrent climate extremes of precipitation deficit and extreme temperature, and assessed the return periods of concurrent climate extremes under the past century, future RCP4.5 and RCP8.5 scenarios.

The survival Kendall regression period (*SKRP*) developed by Salvadori et al. [41] is devoted to overcoming the unboundedness. The critical layer divides the region into safe and dangerous events in such a way that one of the margins may tend to infinity (although the probability is very small). The survival Kendall return period (T_{SKRP}) can be formulated as:

$$T_{SKRP} = \frac{\mu}{1 - \bar{K}(t)} \quad (8)$$

where $\bar{K}(t)$ is the survival Kendall distribution function given by:

$$\bar{K}(t) = P(\bar{F}(x_1, x_2) \geq t) = P(\hat{C}(\bar{F}_1(x), \bar{F}_2(y))) \quad (9)$$

where \hat{C} is the survival copula, and \bar{F}_1 and \bar{F}_2 are the marginal survival distribution functions.

It has been widely addressed that the precipitation and temperature obey a Weibull distribution. The t-copula and Archimedean copula (Frank, Clayton, Gumbel) are assigned to construct a two-dimensional joint distribution, and the parameters of which are estimated by the maximum likelihood method. According to the calculation results of squared Euclidean distance (SED) [42], we selected the t-copula [43] to calculate the bivariate *SKRP*.

2.3.3. Impact of Concurrent Events on the Ecosystem

Droughts have a lagged effect on ecosystems in Southwest China, and droughts in winter and spring can significantly reduce primary productivity in spring and summer [44]. Here, we used NPP and NDVI data to study the effects of concurrent events in October–March on terrestrial ecosystems in spring (March–May) and year-round from 1985 to 2015.

First, based on the monthly NDVI and NPP values, the values within the study region were extracted and the mean or cumulative values were calculated for spring (March–May) and year. Then, we calculated the NDVI and NPP anomalies for each spring and year relative to the mean values for the period from 2000 to 2009. This time period was chosen mainly since the land cover data and vegetation index data used by NPP changed around 2000, and also given that most of the years analyzed were after 2000. Finally, the spatial averages of NDVI and NPP anomalies for each spring and year were calculated by taking the anomalous values within the study region into account.

3. Results

3.1. Accuracy Measurement of CRU TS Datasets

First, an anomaly analysis of the observed data and CRU data relative to 1971–2000 was performed to determine the variability of temperature and precipitation in the study region over the past century (Figure 2). The results show that the average temperature for October–March in the study region has increased significantly over the past 50 years at a rate of 0.22 °C/10a. The overall warming trend over the past 100 years is slower, at 0.04 °C/10a. In addition, there is no significant trend change in the cumulative precipitation for October–March in the study region in the past century. However, the decrease trend of precipitation in the last 30 years is about 21 mm/10a. Therefore, a warm-dry trend is evident in the study region in recent decades.

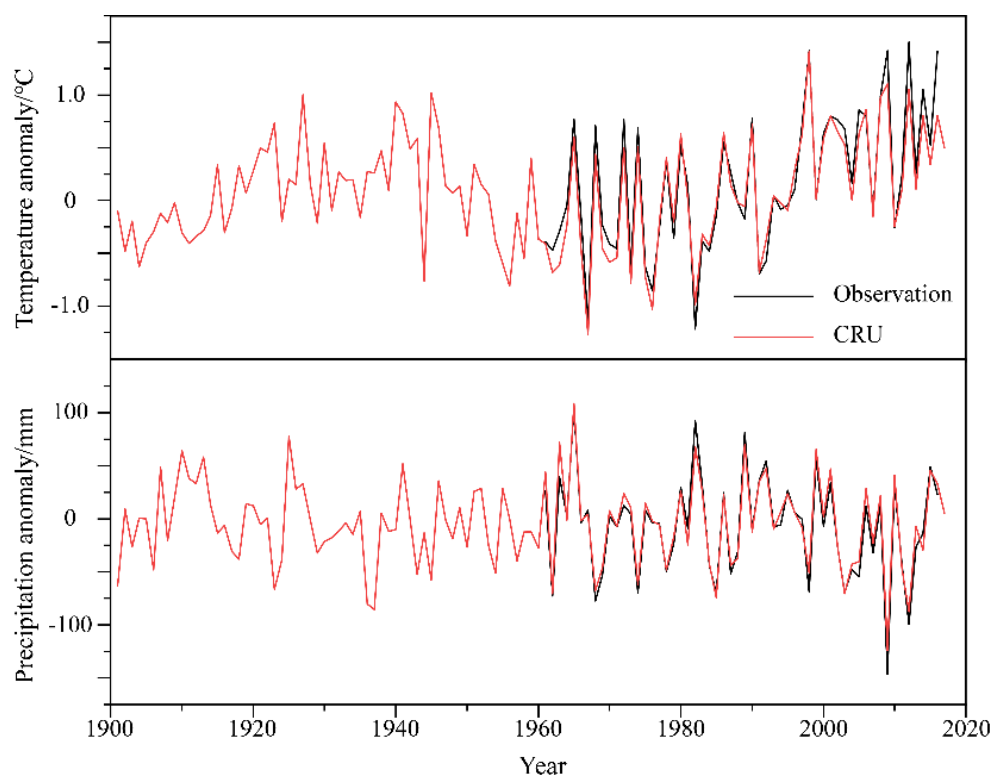


Figure 2. Temperature and precipitation anomalies for October–March relative to the 1971–2000 average in the study region.

RMSE is one of the most commonly used indicators to assess accuracy, and is the expected error of all samples after removing the actual values, which is equivalent to the true error. RMSE values for temperature and precipitation are about 0.18 and 10.47, respectively. The correlation coefficient (Pearson’s R) between the CRU data and the observed data is close to 1 (passing the significance test of 0.01). MAE/MAPE is also the difference between the CRU data and the observed data, which can reflect the magnitude of deviation relative to the original observed data. From the data in Table 1, it can be seen that the CRU data have a small deviation relative to the observed data. These results indicate that the CRU data have relatively good accuracy and desirable regional representativeness. The subsequent analyses were conducted based on CRU data.

Table 1. The scores of each indicator in accuracy measurement.

Indicator	RMSE	R	MAE	MAPE
Temperature	0.18	0.96 *	0.14	0.45%
Precipitation	10.47	0.98 *	8.03	1.26%

* Statistically significant at 0.01 level.

3.2. Return Period of Concurrent Events of Precipitation Deficit and Extreme Temperature

The warm-dry trend of recent decades can be seen in the changes in temperature and precipitation in the study region. With the increase in temperature, the same magnitude of precipitation deficit will have a more serious impact on the natural and social economic system.

During the past hundred years or so, the highest temperature for October–March in the study region occurred in 1998, which was 1.41 °C higher than the average for 1971–2000, and precipitation decreased by about 51.11 mm relative to the average for 1971–2000, ranking 14th among all years with precipitation deficit; the year with the least precipitation for October–March in the study region was 2009, with a decrease of about

124.27 mm relative to the average for 1971–2000, and the temperature was higher than the average for 1971–2000 by 1.10 °C, second only to 1998.

In terms of univariate return periods, for events characterized by precipitation deficit, the return period of the 2009 event is more than 360 years, the return period of the 2012 is around 45 years, and the return period of the 1998 event is less than 10 years; for events characterized by extreme temperature, the return period of the 1998 event is about 180 years, the return period of the 2009 event is around 35 years, and the return period of the 2012 event is about 40 years. These return periods struggle to accurately describe the probability of two extreme events occurring simultaneously, or the probability of one extreme event and another relatively non-extreme event (i.e., temperature extremes and precipitation deficit relatively non-extreme in 1998, or TEPN event; and precipitation deficit extremes and temperature relatively non-extreme in 2009, or PETN event) occurring simultaneously, and the probability of two relatively non-extreme events (i.e., temperature extremes and precipitation deficit relatively non-extreme in 2012, or TNPN event) occurring simultaneously.

The occurrence of such concurrent events will become more common in the context of climate change, so it is necessary to adopt a bivariate approach to determine the return period of concurrent events, accurately predict the probability of occurrence, and lay the foundations for subsequent hazard and risk assessment. The return period results of concurrent events indicate that the PETN event in 2009 has the largest return period of more than 200 years, the TEPN event in 1998 has the second largest return period of about 80 years, and the TNPN event in 2012 also has a return period of about 50 years. There were also five other events with return periods of between 10 and 20 years (Figure 3).

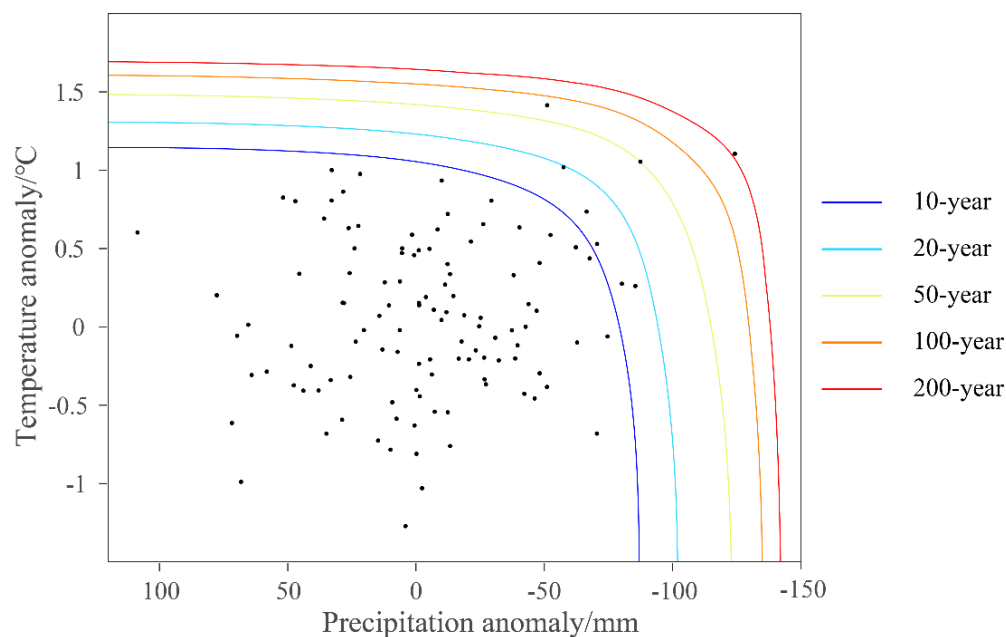


Figure 3. Return period of concurrent events based on CRU data for October–March of 1901–2018 in the study region (10-, 20-, 50-, 100-, and 200-year return periods from the blue to the red isolines, respectively, the same below).

3.3. Impact of Concurrent Events on the Ecosystem

Land use types in Southwest China are dominated by woodland, grassland, and cropland. Climate change and its associated extreme climate events could have important impacts on the greenness and productivity of ecosystems. This study attempts to integrate extreme temperature and precipitation conditions for the purpose of quantifying their impact on ecosystem.

Figure 4 illustrates the impacts of the concurrent events on the greenness of the spring vegetation in the study region. The concurrent event significantly reduced the spring NDVI relative to the average for the period 2000–2009. The NDVI in the spring of 2010, influenced by the PETN event that began in 2009, decreased by a maximum of 50%, with an average decrease of 8.83% within the study region. The NDVI in the spring of 1999, influenced by the TEPN event starting in 1998, decreased by up to 30%, with an average decrease of 5.15% in the study region. The TNPN event starting in 2012 caused a maximum decrease of more than 20% in the NDVI in spring of 2013, with an average decrease of 0.86% in the study region. Spatially, our results suggest that the concurrent events caused widespread vegetation stress in the study region. In spring (March–May), the NDVI exhibited strong negative anomalies across the study area as a result of the concurrent events (Figure 4). The largest negative anomaly in the spring of 2010 occurred in the south-central part of the study region, whereas the largest negative anomalies in the spring of 1999 and the spring of 2013 occurred in the eastern and western parts of the study region, respectively, with lower intensity than that of 2010.

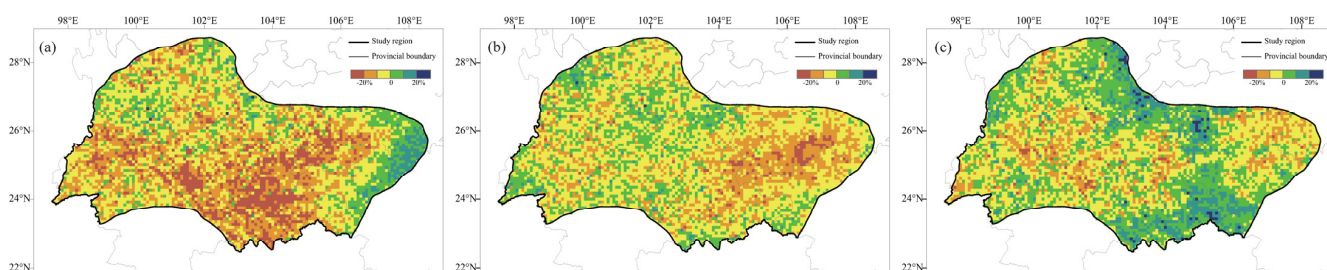


Figure 4. The spatial distributions of NDVI anomaly percentage in the spring (March–May) of 2010 (a), 1999 (b), and 2013 (c) relative to the average for the period 2000–2009.

Similar to the results of NDVI, the concurrent events also significantly reduced spring vegetation productivity within the study region. Relative to the average NPP in spring for the period 2000–2009 in the study region, the NPP in the spring of 2010 decreased by an average of approximately 23% and the total NPP decreased by $10.51 \text{ Tg C a}^{-1}$. The NPP in the spring of 1999 decreased by an average of 10.49%, and the total NPP decreased by 3.48 Tg C a^{-1} . The NPP in the spring of 2013 was an overall positive anomaly with an increase of approximately 3%. The spatial distribution of anomaly percentage of NPP is basically similar to that of NDVI, except for differences in intensity (Figure 5).

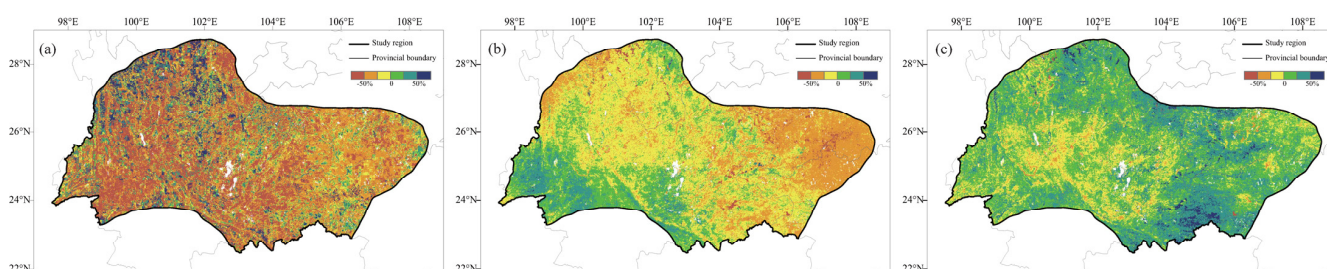


Figure 5. The spatial distributions of NPP anomaly percentage in spring (March–May) of 2010 (a), 1999 (b), and 2013 (c) relative to the average for the period 2000–2009.

When it comes to the distribution of annual NDVI anomaly percentages, the majority of the study region shows weak negative anomalies in annual NDVI due to the lagging effect of concurrent events (Figure 6). Over 63% of the areas showed a decrease in annual NDVI in 2010 compared to the average for the 2000–2009 period, with an average decrease of 2.23% on a regional scale, while nearly 75% of the areas showed a decrease in annual NDVI in 1999, with an average decrease of 1.95% on a regional scale. Half of the areas showed a decrease in the annual NDVI in 2013, with the overall regional scale being in

line with the average. In contrast to the clear trend in spring NDVI with the intensity of concurrent events, the trend in annual NDVI is not as pronounced, partly since annual vegetation greenness is also influenced by summer and autumn weather, and the decline in NDVI in the study region was somewhat mitigated by more precipitation than the same period after August 2010, when temperatures were essentially flat. Spatially, the distribution of annual NDVI anomaly percentages is generally consistent with that of spring, albeit with slightly lower intensity.

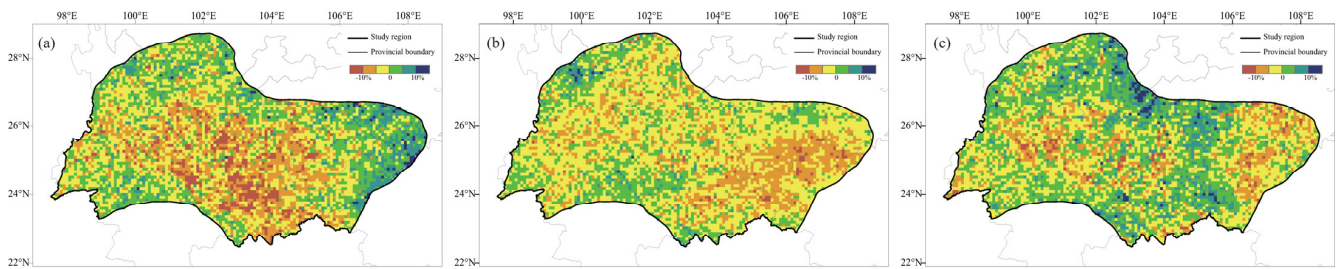


Figure 6. The spatial distributions of annual NDVI anomaly percentage in 2010 (a), 1999 (b), and 2013 (c) relative to the average for the period 2000–2009.

As for the annual NPP anomaly percentages, the decreased amplitude and spatial distribution of NPP in the study region were more consistent with the changes in spring NPP, although the changes in amplitude were slightly smaller (Figure 7). The vast majority of the study region showed a significant decrease in annual NPP in 2010 compared to the average for the 2000–2009 period, with an average decrease of 7.22% on a regional scale, which was the lowest level in the study period. In 1999, the area with a declining trend in annual NPP decreased significantly compared with spring, with an average decrease of 3.30% on a regional scale. The decline trend and amplitude of the annual NPP in 2013 were basically the same as those in spring, with an overall average decrease of 1.05% on a regional scale.

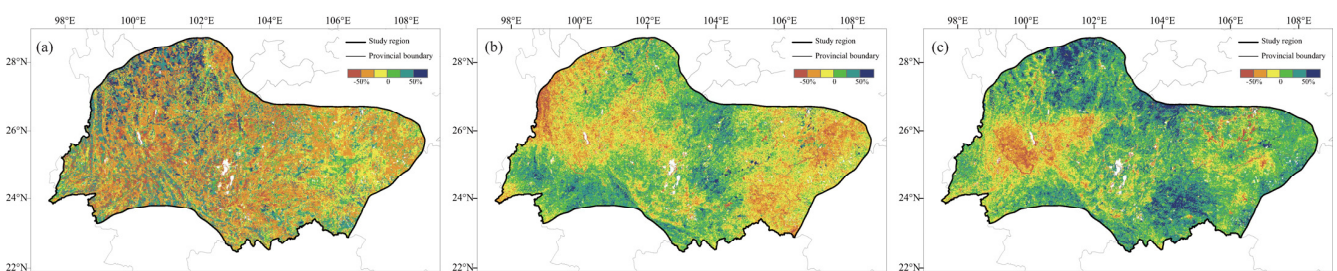


Figure 7. The spatial distributions of annual NPP anomaly percentage in 2010 (a), 1999 (b), and 2013 (c) relative to the average for the period 2000–2009.

3.4. Return Period of Concurrent Events under RCP Scenarios

The assessment of the occurrence and impacts of concurrent events can provide a basis for future research. Here, our analysis leads to the following important question: what will the probability of the occurrence of these three events be in the future, which is an important guide for future ecosystem and socioeconomic risk prediction and adaptation actions. Using the return period calculation method of the concurrent events given in Section 2.3.2, the return periods of concurrent events simulated by the GCMs for the future RCP4.5 and RCP8.5 scenarios were evaluated. The asterisks, pentagrams, and circles in Figures 8 and 9 refer to TEPN events, PETN events, and TNPN events, respectively.

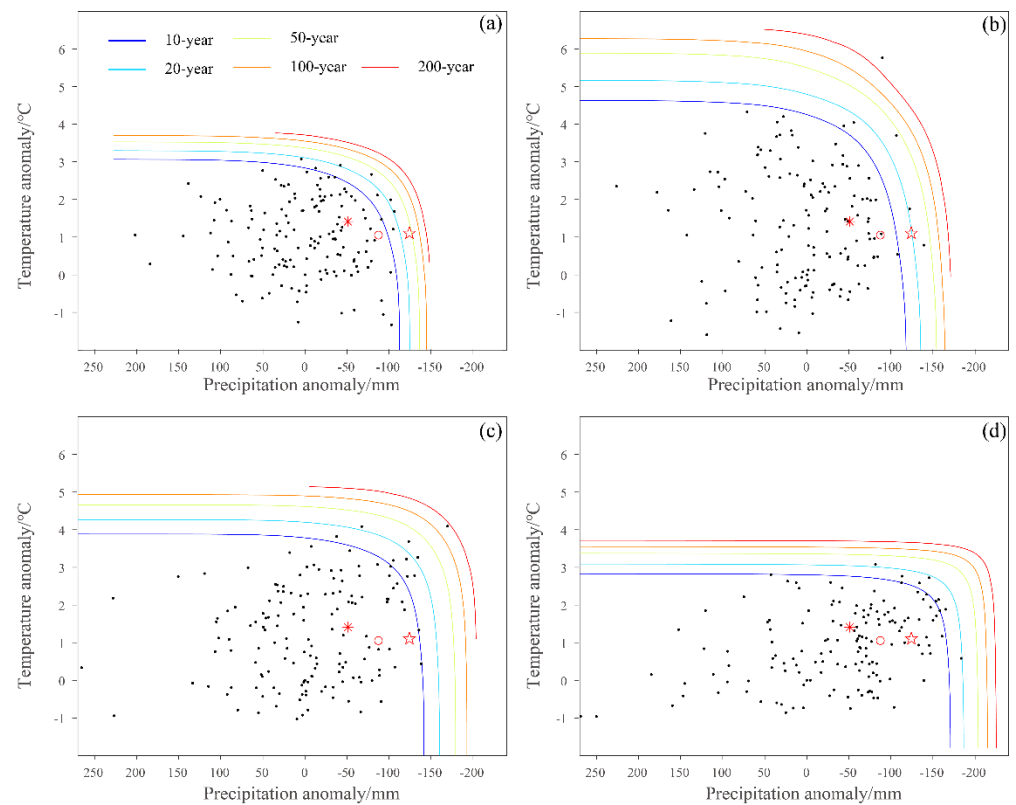


Figure 8. Return period of concurrent events under RCP4.5 scenario for October–March of 1950–2009 in the study region ((a) GFDL-ESM2M; (b) HadGEM2-ES; (c) IPSL-CM5A-LR; (d) NorESM1-M; asterisk indicates TEPN; pentagram indicates PETN; circle indicates TNPN; the same below).

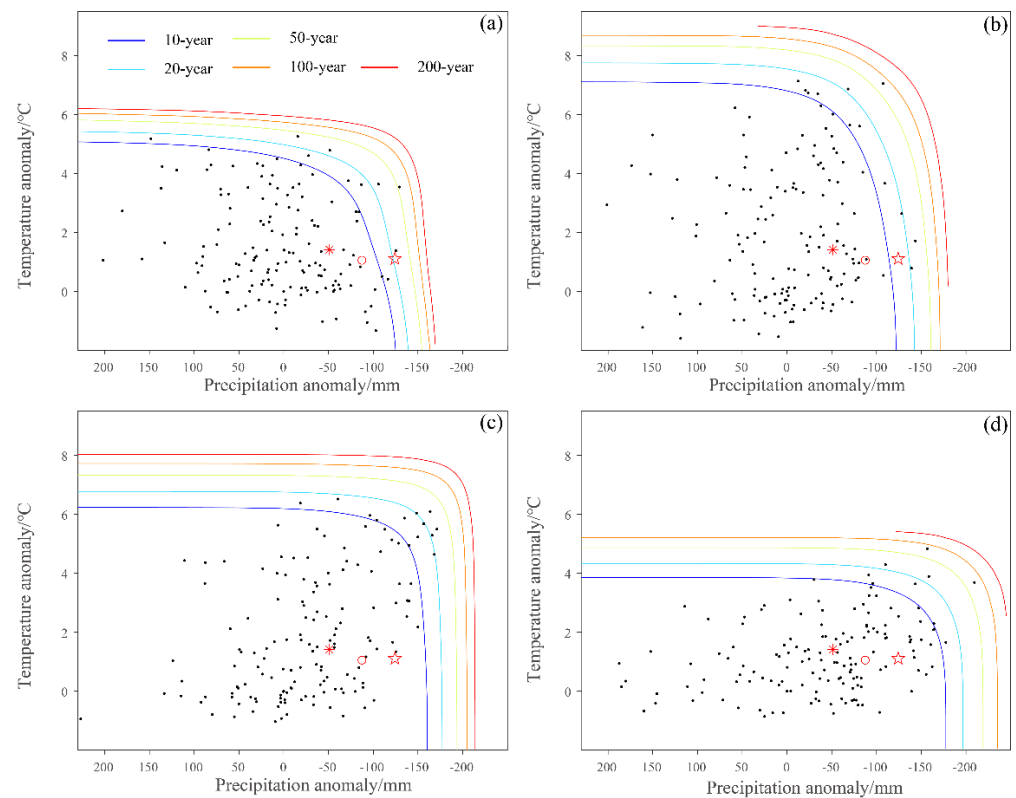


Figure 9. Return period of concurrent events under RCP8.5 scenario for October–March of 1950–2009 in the study region ((a) GFDL-ESM2M; (b) HadGEM2-ES; (c) IPSL-CM5A-LR; (d) NorESM1-M).

Under RCP4.5 scenario, it can be seen from the temperature and precipitation distribution for October–March in the study region simulated by GFDL-ESM2M that the average temperature would increase by about 3 °C relative to the average for the period 1971–2000, and the precipitation deficit would not exceed 124 mm for the PETN event. In this case, both the HEND and TNPN events would have a return period of less than 10 years and become normal events; the return period of the PETN event would be reduced from 200 years to 50 years, and the possibility of occurrence would be greatly increased (Figure 8a). In the temperature simulated by HADGEM2-ES, an extreme value of 6 °C would exceed the average for the period 1971–2000, and the magnitude of precipitation deficit would be similar to that of the PETN event. In this case, HEND and TNPN events would also become normal events; the recurrence period of PETN events would be significantly reduced to about 20 years, and the possibility of occurrence would be further increased. It is worth mentioning that the precipitation deficit of the PETN event with a return period close to 50 years would be about 140 mm, and the temperature increase would be less than 1 °C (Figure 8b). Temperature and precipitation changes simulated by IPSL-CM5A-LR and NorESM1-M would be similar, with a 4 °C (Figure 8c) or 3 °C (Figure 8d) temperature increase and a precipitation deficit close to 200 mm compared to the average of the period 1971–2000. In both cases, TEPN, PETN, and TNPN events would become normal events. The study region would experience more severe temperature increase and precipitation deficit events.

Under RCP8.5 scenario, compared with the average for the period 1971–2000, the maximum precipitation deficit simulated by GFDL-ESM2M and HADGEM2-ES would be about 150 mm; the difference lies in that the temperature increase simulated by GFDL-ESM2M would be about 5 °C, while the temperature increase simulated by HADGEM2-ES would be over 7 °C. In both cases, TEPN and PETN events would become normal events; the return period for PETN events would be reduced to 20 years (Figure 9a) and less than 20 years (Figure 9b). Compared with the average for the period 1971–2000, the maximum precipitation deficit simulated by IPSL-CM5A-LR and NorESM1-M would be similar, both around 200 mm, and the temperature increase simulated by IPSL-CM5A-LR would be around 6 °C higher than that of NorESM1-M by about 5 °C. In both cases, TEPN, PETN and PETN events would become normal events. A significant increase in temperature would result in a return period of only about 20 years for extreme events with a precipitation deficit of about 150 mm (Figure 9c,d).

4. Discussion

Studies have shown that global warming and the other changes in the climate system triggered by it are unprecedented over decades and even millennia. The changes in the climate system have led to the accentuation of the adverse effects of gradual events and the frequency of extreme weather and climate events (emergencies) [45], which have posed significant risks to natural and human systems on all continents and oceans, severely affecting the dynamics of ecosystems. Southwest China is a key ecologically vulnerable region, and the frequent occurrence of extreme climatic events in recent years [46] has seriously affected the regional ecological security pattern [47]. Previous studies have shown that the correlation between vegetation cover changes and temperature factors is more significant in most parts of Southwest China, that extreme temperature events have a greater impact on ecosystems than extreme precipitation events, and that research on the impact of extreme events on ecosystems should focus more on the increasing frequency and impact of extreme precipitation and extreme temperature in the region [48,49]. Therefore, it is necessary to study the frequency of concurrent events and their effects on the spatial and temporal dynamic patterns of ecosystems in Southwest China through a comprehensive analysis of multi-climatic elements to provide theoretical references for the sustainable development and conservation of ecosystems in the region.

Return periods are a useful tool for assessing the risk of extreme events, but single-factor return periods can significantly overestimate or underestimate the frequency of

extreme events, and analysis of concurrent events return periods is essential for quantifying ecosystem responses to climate factors and can better explain the dynamics of temperature and precipitation in relation to ecosystem change. The correlation coefficient between the temperature values of the CRU data used in this study and the observed values is 0.96, with a coefficient of determination above 0.92; the correlation coefficient between the precipitation values and the observed values is 0.98, with a coefficient of determination above 0.95. This indicates that the CRU data have high accuracy in characterizing both temperature and precipitation changes in Southwest China. The discrepancy mainly lies in the poor consistency of the extremes, which is mainly reflected in the underestimation of the temperature in 2009, 2012, and 2016 and the overestimation of the precipitation deficit in 1998, 2009, and 2012, which may underestimate the return period of concurrent events. The results of the spatial correlation analysis based on ArcGIS version 10.2 show an overall positive correlation between NPP and NDVI in Southwest China on seasonal and interannual scales, which can also be seen in the more consistent adverse effects of concurrent events on both. In addition, the impact model established in this study mainly focuses on regional averages, and future dynamical mechanism analysis can be conducted for spatial differences caused by three extreme events (TEPN, PETN, and TNPN) to explore the possible processes of different extreme events affecting ecosystems.

The risk of climate-related impacts results from the interaction of climate-related hazards (including hazardous events and trends) with the vulnerability and exposure of human and natural systems [50]. Therefore, climate-related hazards include climate change trends and extreme events, both of which have the potential to affect ecosystems to different degrees. Impact assessment of climate change trends could introduce the concept of thresholds to estimate the extent of ecosystem risk by comparing indicators over different periods [51,52]. For extreme events, impact or risk assessment generally considers three elements: hazard, vulnerability, and exposure; hazard is the probability of occurrence of extreme events, and exposure is the ecosystem itself; vulnerability refers to the degree of destruction to exposure by the occurrence of extreme events, and is the probability of damage to nature and socio-economics within the influence of the hazard. The return period of concurrent events can be used as a measure of hazard, the impact model can provide criteria for vulnerability, and the spatial and temporal distribution of ecosystem indicators simulated by the ecological model can be used as exposure (that is, the ecosystem risk of concurrent events can be quantitatively assessed). This can provide useful ideas for further revealing and separating the effects of climate trends and extreme events on ecosystems.

In this study, the univariate return periods calculated using the Pearson Type III Distribution are shown in Figure S1. From the results, it is clear that the precipitation-based univariate hazard estimation approaches significantly overestimate the return period (hazard of occurrence) of concurrent events in 2009 and underestimate the return period (hazard of occurrence) of concurrent events in 1998 and 2012. The temperature-based univariate hazard estimation approaches underestimate the return period (hazard of occurrence) of all three concurrent events. Based on the results of the variation trends of vegetation greenness and productivity decline and the return period of concurrent events in this study, a relationship curve of concurrent events affecting ecosystems can be established as an indicator of vulnerability in the risk assessment of extreme events. Here, it is reasonable to assume that the larger the return period of concurrent events, the greater the NDVI and NPP reduction rate. The return periods of different concurrent events and the corresponding NDVI and NPP anomaly percentages were counted, and the quantitative relationship between concurrent events and their corresponding NDVI and NPP anomaly percentages was established by linear regression methods to quantitatively assess the impact of concurrent events with different return periods on the ecosystem (Figure S2). The results show that for every 10-year increase in the return period of concurrent climate extremes, NDVI and NPP decrease by 0.4% and 1.6%, respectively. It should be noted that the purpose of constructing the vulnerability curves in this study is to propose a

feasible method for vulnerability assessment. However, due to the limitation of the amount of data, only four events were used for the construction of the curves. With the increase in the amount of data, more accurate results may be obtained in subsequent studies.

5. Conclusions

In this study, the return periods of past and future concurrent events of precipitation deficit and extreme temperature for October–March in Southwest China were evaluated. Based on this, the spatial and temporal dynamic patterns of the impacts of concurrent events on the ecosystem were explored. The conclusions are as follows:

(1) There has been a significant warm-dry trend in Southwest China over the past hundred years or so, especially in recent decades. In this context, the possibility of simultaneous high temperature and precipitation deficit events has increased significantly. The return periods of the concurrent extreme precipitation non-extreme heat event in 2009, the concurrent extreme heat non-extreme precipitation event in 1998, and the concurrent non-extreme heat non-extreme precipitation event 2012 are about 200, 80, and 50 years, respectively.

(2) Concurrent events severely impacted terrestrial ecosystems in Southwest China, significantly reducing vegetation greenness and primary productivity. The results show that concurrent events caused the decrease in NDVI and NPP for the spring and year. Reductions in NDVI and NPP relative to the average for the 2000–2009 period increased with the intensity of the concurrent events. Concurrent events with the 200-year return period reduced spring NDVI and NPP by 8.8% and 23%, and annual NDVI and NPP by 2.23% and 7.22%, respectively.

(3) Concurrent events are expected to become more frequent and severe in the context of climate change. The analysis results of climate scenarios indicate that the faster the temperature increases in Southwest China, the more pronounced the shortening of the return period of concurrent events is. Under RCP4.5 and RCP8.5 scenarios, the return period of the PETN events defined in this study would shorten from 200 years to less than 50 and 20 years, respectively, and the return period of both TEPN and TNPN events would be less than 10 years, becoming non-extreme events.

Supplementary Materials: The following are available online at: <https://www.mdpi.com/article/10.3390/rs14071678/s1>, Figure S1: Precipitation-based and temperature-based univariate return period in Southwest China and their corresponding years; Figure S2: The quantitative relationship between return period of concurrent events and NDVI and NPP anomaly percentages.

Author Contributions: Conceptualization, J.G. and L.L.; methodology, L.L., A.F., K.J. and Y.L.; software, L.L., L.Z. and R.Y.; validation, J.G., A.F., K.J. and S.W.; writing—original draft preparation, L.L. and Y.J.; writing—review and editing, J.G.; supervision, J.G. and S.W. All authors have read and agreed to the published version of the manuscript.

Funding: This research was funded by the National Key Research and Development Program of China [Grant number 2018YFC1508801, 2018YFC1508900]; the National Natural Science Foundation of China [Grant number 42101311, 42071288]; the China Postdoctoral Science Foundation [Grant number 2021M670433]; and the Programme of Kezhen-Bingwei Excellent Young Scientists of the Institute of Geographic Sciences and Natural Resources Research, Chinese Academy of Sciences [Grant number 2020RC002].

Institutional Review Board Statement: Not applicable.

Informed Consent Statement: Not applicable.

Data Availability Statement: Publicly available datasets were analyzed in this study.

Acknowledgments: The authors acknowledge Amir AghaKouchak for providing the code for the Survival Copula Multivariate Return period, and the GIMMS group for producing and sharing the NDVI dataset, and the Global Change Research Data Publishing & Repository for producing and sharing the NPP dataset, and the China Meteorological Data Service Center and the CRU for

providing the climatic data. Thanks to the editor and the anonymous reviewers for improving this paper significantly.

Conflicts of Interest: The authors declare no conflict of interest.

References

- Jonas, S.; Fronczyk, K.; Pratt, L. A Framework to Understand Extreme Space Weather Event Probability. *Risk. Anal.* **2018**, *38*, 1534–1540. [[CrossRef](#)]
- Jehanzaib, M.; Sattar, M.; Lee, J.; Kim, T. Investigating effect of climate change on drought propagation from meteorological to hydrological drought using multi-model ensemble projections. *Stoch. Environ. Res. Risk Assess.* **2020**, *34*, 7–21. [[CrossRef](#)]
- Cardell, M.F.; Amengual, A.; Romero, R.; Ramis, C. Future extremes of temperature and precipitation in Europe derived from a combination of dynamical and statistical approaches. *Int. J. Climatol.* **2020**, *40*, 4800–4827. [[CrossRef](#)]
- Cohen, J.; Fink, D.; Zuckerberg, B. Avian responses to extreme weather across functional traits and temporal scales. *Glob. Chang. Biol.* **2020**, *26*, 4240–4250. [[CrossRef](#)]
- Weilhammer, V.; Schmid, J.; Mittermeier, I.; Schreiber, F.; Jiang, L.; Pastuhovic, V.; Herr, C.; Heinze, S. Extreme weather events in Europe and their health consequences—A systematic review. *Int. J. Hyg. Environ. Health* **2021**, *233*, 113688. [[CrossRef](#)]
- Nanzad, L.; Zhang, J.; Tuvdendorj, B.; Yang, S.; Rinzin, S.; Prodhon, F.; Sharma, T. Assessment of Drought Impact on Net Primary Productivity in the Terrestrial Ecosystems of Mongolia from 2003 to 2018. *Remote Sens.* **2021**, *13*, 2522. [[CrossRef](#)]
- Li, J.; Wang, Y.; Liu, L. Responses of the Terrestrial Ecosystem Productivity to Droughts in China. *Front. Earth Sci.* **2020**, *8*, 59. [[CrossRef](#)]
- Guerrero-Meseguer, L.; Marin, A.; Sanz-Lazaro, C. Heat wave intensity can vary the cumulative effects of multiple environmental stressors on *Posidonia oceanica* seedlings. *Mar. Environ. Res.* **2020**, *159*, 105001. [[CrossRef](#)]
- Ainsworth, T.D.; Hurd, C.L.; Gates, R.D.; Boyd, P.W. How do we overcome abrupt degradation of marine ecosystems and meet the challenge of heat waves and climate extremes? *Glob. Chang. Biol.* **2020**, *26*, 343–354. [[CrossRef](#)]
- He, B.; Liu, J.; Guo, L.; Wu, X.; Xie, X.; Zhang, Y.; Chen, C.; Zhong, Z.; Chen, Z. Recovery of ecosystem carbon and energy fluxes from the 2003 drought in Europe and the 2012 drought in the United States. *Geophys. Res. Lett.* **2018**, *45*, 4879–4888. [[CrossRef](#)]
- Rustad, L.E. The response of terrestrial ecosystems to global climate change: Towards an integrated approach. *Sci. Total Environ.* **2008**, *404*, 222–235. [[CrossRef](#)]
- Jones, C.; Lowe, J.; Liddicoat, S.; Betts, R. Committed terrestrial ecosystem changes due to climate change. *Nat. Geosci.* **2009**, *2*, 484–487. [[CrossRef](#)]
- Ding, Z.; Liu, Y.; Wang, L.; Chen, Y.; Yu, P.; Ma, M.; Tang, X. Effects and implications of ecological restoration projects on ecosystem water use efficiency in the karst region of Southwest China. *Ecol. Eng.* **2021**, *170*, 106356. [[CrossRef](#)]
- Li, S.; Liu, C.; Chen, J.; Wang, S. Karst ecosystem and environment: Characteristics, evolution processes, and sustainable development. *Agric. Ecosyst. Environ.* **2021**, *306*, 107173. [[CrossRef](#)]
- Phillips, J.D. Biogeomorphology and contingent ecosystem engineering in karst landscapes. *Prog. Phys. Geogr.-Earth Environ.* **2016**, *40*, 503–526. [[CrossRef](#)]
- Guo, F.; Jiang, G.; Yuan, D.; Polk, J.S. Evolution of major environmental geological problems in karst areas of Southwestern China. *Environ. Earth Sci.* **2013**, *69*, 2427–2435. [[CrossRef](#)]
- Li, M.; Yin, L.; Zhang, Y.; Su, X.; Liu, G.; Wang, X.; Au, Y.; Wu, X. Spatio-temporal dynamics of fractional vegetation coverage based on MODIS-EVI and its driving factors in Southwest China. *Acta Ecol. Sin.* **2021**, *41*, 1138–1147.
- Zhang, M.; He, J.; Wang, B.; Wang, S.; Li, S.; Liu, W.; Ma, X. Extreme drought changes in Southwest China from 1960 to 2009. *J. Geogr. Sci.* **2013**, *23*, 3–16. [[CrossRef](#)]
- Zhang, W.; Jin, F.; Zhao, J.; Qi, L.; Ren, H. The possible influence of a nonconventional El Niño on the severe autumn drought of 2009 in Southwest China. *J. Clim.* **2013**, *26*, 8392–8405. [[CrossRef](#)]
- Li, X.; Li, Y.; Chen, A.; Gao, M.; Slette, I.; Piao, S. The impact of the 2009/2010 drought on vegetation growth and terrestrial carbon balance in Southwest China. *Agric. For. Meteorol.* **2019**, *269*, 239–248. [[CrossRef](#)]
- Brunetti, M.; Maugeri, M.; Nanni, T. Changes in total precipitation, rainy days and extreme events in northeastern Italy. *Int. J. Climatol.* **2001**, *21*, 861–871. [[CrossRef](#)]
- England, J., Jr.; Salas, J.; Jarrett, R. Comparisons of two moments-based estimators that utilize historical and paleoflood data for the log Pearson type III distribution. *Water Resour. Res.* **2003**, *39*, 1243. [[CrossRef](#)]
- Ayantobo, O.; Li, Y.; Song, S.; Yao, N. Spatial comparability of drought characteristics and related return periods in mainland China over 1961–2013. *J. Hydrol.* **2017**, *550*, 549–567. [[CrossRef](#)]
- Gräler, B.; Van Den Berg, M.; Vandenberghe, S.; Petroselli, A.; Grimaldi, S.; Baets, B.; Verhoest, N. Multivariate return periods in hydrology: A critical and practical review focusing on synthetic design hydrograph estimation. *Hydrol. Earth Syst. Sci.* **2013**, *17*, 1281–1296. [[CrossRef](#)]
- Li, Y.; Ren, F.; Li, Y.; Wang, P.; Yan, H. Characteristics of the regional meteorological drought events in Southwest China during 1960–2010. *J. Meteorol. Res.* **2014**, *28*, 381–392. [[CrossRef](#)]
- Huang, Y.; Xu, C.; Yang, H.; Wang, J.; Jiang, D.; Zhao, C. Temporal and spatial variability of droughts in Southwest China from 1961 to 2012. *Sustainability* **2015**, *7*, 13597–13609. [[CrossRef](#)]

27. Wang, L.; Chen, W.; Zhou, W.; Huang, G. Drought in Southwest China: A Review. *Atmos. Ocean. Sci. Lett.* **2015**, *8*, 339–344.
28. Huang, R.; Liu, Y.; Wang, L.; Wang, L. Analyses of the Causes of Severe Drought Occurring in Southwest China from the Fall of 2009 to the Spring of 2010. *Chin. J. Atmos. Sci.* **2012**, *36*, 443–457.
29. Wang, L.; Chen, W.; Zhou, W. Assessment of future drought in Southwest China based on CMIP5 multimodel projections. *Adv. Atmos. Sci.* **2014**, *31*, 1035–1050. [[CrossRef](#)]
30. Tang, H.; Wen, T.; Shi, P.; Qu, S.; Zhao, L.; Li, Q. Analysis of Characteristics of Hydrological and Meteorological Drought Evolution in Southwest China. *Water* **2021**, *13*, 1846. [[CrossRef](#)]
31. Harris, I.; Osborn, T.; Jones, P.; Lister, D. Version 4 of the CRU TS monthly high-resolution gridded multivariate climate dataset. *Sci. Data* **2020**, *7*, 1–18. [[CrossRef](#)] [[PubMed](#)]
32. Warszawski, L.; Frieler, K.; Huber, V.; Piontek, F.; Serdeczny, O.; Schewe, J. The inter-sectoral impact model intercomparison project (ISI-MIP): Project framework. *Proc. Natl. Acad. Sci. USA* **2014**, *111*, 3228–3232. [[CrossRef](#)] [[PubMed](#)]
33. Chen, P.; Shang, J.; Qian, B.; Jing, Q.; Liu, J. A new regionalization scheme for effective ecological restoration on the Loess Plateau in China. *Remote Sens.* **2017**, *9*, 1323. [[CrossRef](#)]
34. Huang, L.; Ning, J.; Zhu, P.; Zheng, Y.; Zhai, J. The conservation patterns of grassland ecosystem in response to the forage-livestock balance in North China. *J. Geogr. Sci.* **2021**, *31*, 518–534. [[CrossRef](#)]
35. Jiao, K.; Gao, J.; Liu, Z. Precipitation Drives the NDVI Distribution on the Tibetan Plateau While High Warming Rates May Intensify Its Ecological Droughts. *Remote Sens.* **2021**, *13*, 1305. [[CrossRef](#)]
36. Zhao, Y.; Zhu, J.; Xu, Y. Establishment and assessment of the grid precipitation datasets in China for the past 50 years. *J. Meteorol. Sci.* **2014**, *34*, 414–420.
37. Gupta, H.V.; Kling, H.; Yilmaz, K.K.; Martinez, G.F. Decomposition of the mean squared error and NSE performance criteria: Implications for improving hydrological modelling. *J. Hydrol.* **2009**, *377*, 80–91. [[CrossRef](#)]
38. Gilewski, P. Impact of the Grid Resolution and Deterministic Interpolation of Precipitation on Rainfall-Runoff Modeling in a Sparsely Gauged Mountainous Catchment. *Water* **2021**, *13*, 230. [[CrossRef](#)]
39. AghaKouchak, A.; Cheng, L.; Mazdiyasn, O.; Farahmand, A. Global warming and changes in risk of concurrent climate extremes: Insights from the 2014 California drought. *Geophys. Res. Lett.* **2014**, *41*, 8847–8852. [[CrossRef](#)]
40. Sklar, A. Random variables, distribution functions, and copulas: A personal look backward and forward. *Lect. Notes-Monogr. Ser.* **1996**, *28*, 1–14.
41. Salvadori, G.; Durante, F.; De Michele, C. Multivariate return period calculation via survival functions. *Water Resour. Res.* **2013**, *49*, 2308–2311. [[CrossRef](#)]
42. Hossain, M.; Abufardeh, S. A New Method of Calculating Squared Euclidean Distance (SED) Using pTree Technology and Its Performance Analysis. *EPiC Ser. Comput.* **2019**, *58*, 45–54.
43. Nelsen, R. *An Introduction to Copulas*; Springer: New York, NY, USA, 2007.
44. Zhang, L.; Xiao, J.; Li, J.; Wang, K.; Lei, L.; Guo, H. The 2010 spring drought reduced primary productivity in southwestern China. *Environ. Res. Lett.* **2012**, *7*, 045706. [[CrossRef](#)]
45. IPCC. *Managing the Risks of Extreme Events and Disasters to Advance Climate Change Adaptation: A Special Report of Working Groups I and II of the Intergovernmental Panel on Climate Change*; Cambridge University Press: New York, NY, USA; Cambridge, UK, 2012.
46. Liu, M.; Xu, X.; Sun, A.; Wang, K.; Liu, W.; Zhang, X. Is southwestern China experiencing more frequent precipitation extremes? *Environ. Res. Lett.* **2014**, *9*, 064002. [[CrossRef](#)]
47. Song, L.; Li, Y.; Ren, Y.; Wu, X.; Guo, B.; Tang, X.; Shi, W.; Ma, M.; Han, X.; Zhao, L. Divergent vegetation responses to extreme spring and summer droughts in Southwestern China. *Agric. For. Meteorol.* **2019**, *279*, 107703. [[CrossRef](#)]
48. Zhou, J.; Ma, M.; Xiao, Q.; Wen, J. Vegetation Dynamics and Its Relationship with Climatic Factors in Southwestern China. *Remote Sens. Technol. Appl.* **2017**, *32*, 966–972.
49. Shao, H.; Zhang, Y.; Gu, F.; Shi, C.; Miao, N.; Liu, S. Impacts of climate extremes on ecosystem metrics in southwest China. *Sci. Total Environ.* **2021**, *776*, 145979. [[CrossRef](#)]
50. IPCC. *Climate Change 2014: Impacts, Adaptation, and Vulnerability*; Cambridge University Press: New York, NY, USA; Cambridge, UK, 2014.
51. Gao, J.; Jiao, K.; Wu, S.; Ma, D.; Zhao, D.; Yin, Y.; Dai, E. Past and future effects of climate change on spatially heterogeneous vegetation activity in China. *Earth's Future* **2017**, *5*, 679–692. [[CrossRef](#)]
52. Wu, S.; Liu, L.; Gao, J.; Wang, W. Integrate Risk from Climate Change in China Under Global Warming of 1.5 and 2.0 °C. *Earth's Future* **2019**, *7*, 1307–1322. [[CrossRef](#)]